

Nuclear forces and their impact on structure, reactions and astrophysics

Dick Furnstahl
Ohio State University

July, 2013

Lectures for Week 3

- M.** Many-body problem and basis considerations (as);
Many-body perturbation theory (rjf)
- T.** Neutron matter and astrophysics (as); Operators (rjf)
- W.** Nuclear matter (rjf); Student presentations
- Th.** Impact on (exotic) nuclei (as); Student presentations
- F.** Impact on fundamental symmetries (as); From forces to density functionals (rjf)

Outline

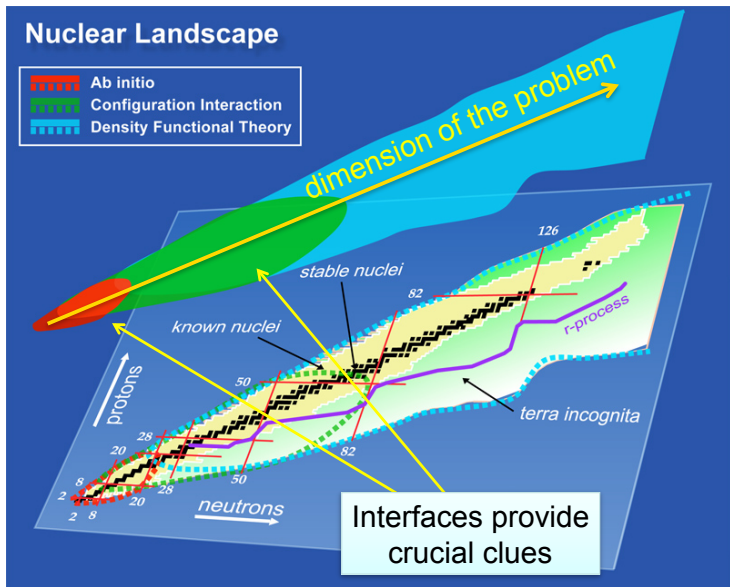
Many-body methods: Selected results

Dilute, natural, Fermi system

Bethe-Brueckner-Goldstone Power Counting

Teaser for MBPT applied in finite nuclei

Overlapping theory methods cover all nuclei





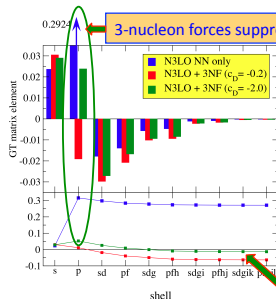
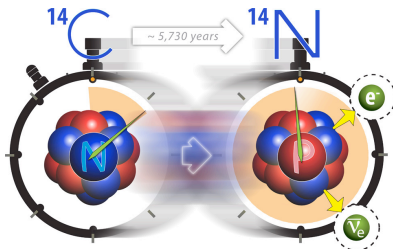
“Why does Carbon-14 live so long?”

Carbon-14 dating relies on $\sim 5,730$ year half-life, but other light nuclei undergo similar beta decay with half-lives less than a day!



UNEDF SciDAC Collaboration
Universal Nuclear Energy Density Functional

- Members of UNEDF collaboration made microscopic nuclear structure calculations to solve the puzzle
- Used systematic chiral Hamiltonian from low-energy effective field theory of QCD
- **Key feature: consistent 3-nucleon interactions**



3-nucleon forces suppress critical component compared to 2-nucleon forces only

- Solutions of ^{14}C and ^{14}N through Hamiltonian diagonalization
- 100-fold reduction in Gamow-Teller transition matrix element

Calculations enabled by high-performance computing through INCITE program

- Dimension of matrix solved for 8 lowest states: $\sim 1 \times 10^9$
- Solution took ~ 6 hours on 215,000 cores on Cray XT5 Jaguar at ORNL



net decay rate is very small

Science ref.: Physical Review Letters **106**, 202502 (2011)
Computational ref.: Procedia Computer Science **1**, 97 (2010)

Coupled cluster method [from D. Dean, G. Hagen, T. Papenbrock]

Asymmetry dependence and spectroscopic factors

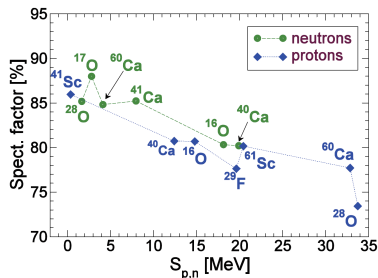
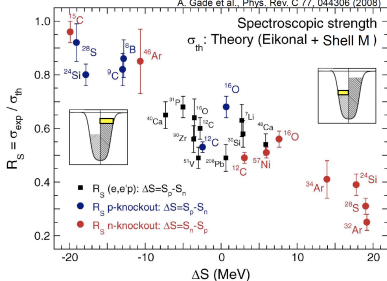
- Spectroscopic factors are not observables
- They are extracted from a cross section based on a specific structure and reaction model
- Structure and reaction models need to be consistent!

Theoretical cross section:

$$\sigma(j^\pi) = \left(\frac{A}{A-1} \right)^N C^2 S(j^\pi) \sigma_{sp}(j, S_N + E_x[j^\pi])$$

Structure theory Reaction theory

A. Gade et al., Phys. Rev. C 77, 044306 (2008)

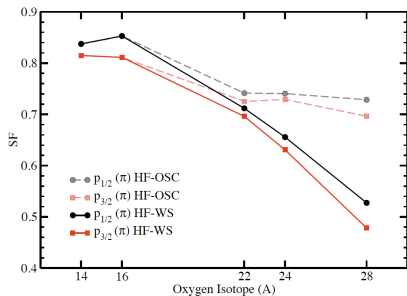


C. Barbieri, W.H. Dickhoff, Int. Jour. Mod. Phys. A24, 2060 (2009).

Self-consistent green's function method show rather weak asymmetry dependence for the spectroscopic factor.

Coupled cluster method [from D. Dean, G. Hagen, T. Papenbrock]

Quenching of spectroscopic factors for proton removal in neutron rich oxygen isotopes



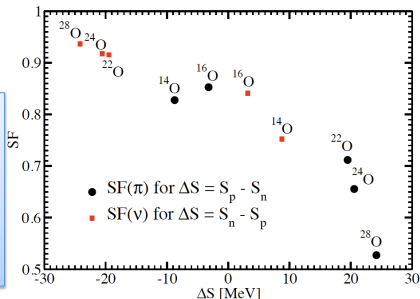
Strong asymmetry dependence on the SF for proton and neutron removal in neutron rich oxygen isotopes.

SF \sim 1 for neutron removal while protons are strongly correlated SF \sim 0.6-0.7 in $^{22,24,28}\text{O}$

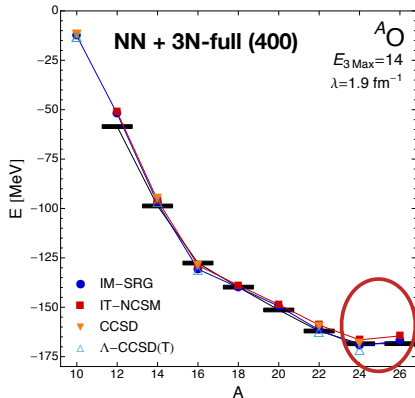
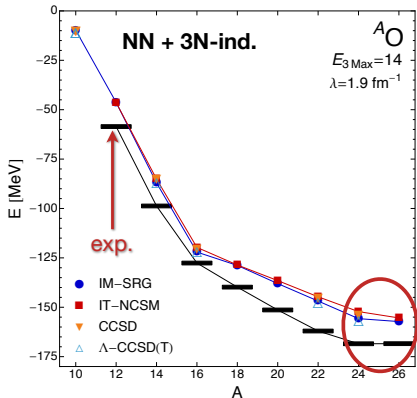
Spectroscopic factor is a useful tool to study correlations towards the dripline.

SF for proton removal in neutron rich ^{24}O show strong “quenching” pointing to large deviations from a mean-field like picture.

G. Hagen et al Phys. Rev. Lett. 107, 032501 (2011).



Oxygen chain with multi-reference IM-SRG [H. Hergert]

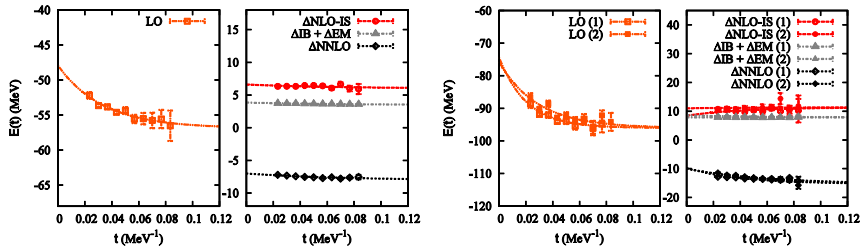


- ref. state: number-projected Hartree-Fock-Bogoliubov vacuum
- results (mostly) insensitive to choice of generator for same H^{od}
- consistency between different many-body methods

Ground states of ^8Be and ^{12}C [E. Epelbaum]

E.E., Krebs, Lee, Meißner, PRL 106 (11) 192501

Simulations for ^8Be and ^{12}C , $L=11.8$ fm



Ground state energies ($L=11.8$ fm) of ^4He , ^8Be , ^{12}C & ^{16}O

	^4He	^8Be	^{12}C	^{16}O
LO [Q^0], in MeV	-28.0(3)	-57(2)	-96(2)	-144(4)
NLO [Q^2], in MeV	-24.9(5)	-47(2)	-77(3)	-116(6)
NNLO [Q^3], in MeV	-28.3(6)	-55(2)	-92(3)	-135(6)
Experiment, in MeV	-28.30	-56.5	-92.2	-127.6

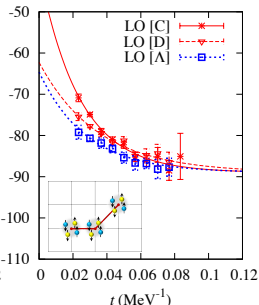
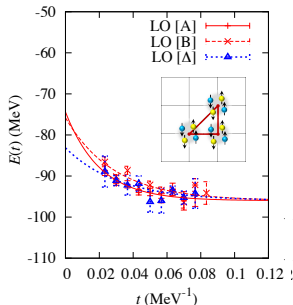
Hoyle State [E. Epelbaum]

EE, Krebs, Lähde, Lee, Meißner, PRL 106 (2011) 192501; PRL 109 (2012) 252501

Lattice results for low-lying even-parity states of ^{12}C

	0_1^+	$2_1^+(E^+)$	0_2^+	$2_2^+(E^+)$
LO	-96(2)	-94(2)	-89(2)	-88(2)
NLO	-77(3)	-74(3)	-72(3)	-70(3)
NNLO	-92(3)	-89(3)	-85(3)	-83(3)
Exp	-92.16	-87.72	-84.51	-82(1)

Probing (α -cluster) structure of the 0_1^+ , 0_2^+ states



RMS radii and quadrupole moments

	LO	Experiment
$r(0_1^+)$ [fm]	2.2(2)	2.47(2) [26]
$r(2_1^+)$ [fm]	2.2(2)	—
$Q(2_1^+)$ [$e \text{ fm}^2$]	6(2)	6(3) [27]
$r(0_2^+)$ [fm]	2.4(2)	—
$r(2_2^+)$ [fm]	2.4(2)	—
$Q(2_2^+)$ [$e \text{ fm}^2$]	-7(2)	—

Outline

Many-body methods: Selected results

Dilute, natural, Fermi system

Bethe-Brueckner-Goldstone Power Counting

Teaser for MBPT applied in finite nuclei

EFT for “Natural” Short-Range Interaction

- A simple, general interaction is a sum of delta functions and derivatives of delta functions. In momentum space,

$$\langle \mathbf{k} | V_{\text{eft}} | \mathbf{k}' \rangle = C_0 + \frac{1}{2} C_2 (\mathbf{k}^2 + \mathbf{k}'^2) + C_2' \mathbf{k} \cdot \mathbf{k}' + \dots$$

- Or, \mathcal{L}_{eft} has most general local (contact) interactions:

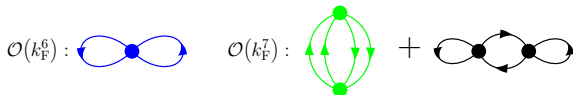
$$\begin{aligned} \mathcal{L}_{\text{eft}} = & \psi^\dagger \left[i \frac{\partial}{\partial t} + \frac{\vec{\nabla}^2}{2M} \right] \psi - \frac{C_0}{2} (\psi^\dagger \psi)^2 + \frac{C_2}{16} [(\psi \psi)^\dagger (\psi \overleftrightarrow{\nabla}^2 \psi) + \text{h.c.}] \\ & + \frac{C_2'}{8} (\psi \overleftrightarrow{\nabla} \psi)^\dagger \cdot (\psi \overleftrightarrow{\nabla} \psi) - \frac{D_0}{6} (\psi^\dagger \psi)^3 + \dots \end{aligned}$$

- Dimensional analysis $\implies C_{2i} \sim \frac{4\pi}{M} R^{2i+1}$, $D_{2i} \sim \frac{4\pi}{M} R^{2i+4}$

Effective Field Theory Ingredients

Ref: Hammer, rjf [nucl-th/0702040]

- 1** Use the most general \mathcal{L} with low-energy dof's consistent with global and local symmetries of underlying theory
 - $\mathcal{L}_{\text{eft}} = \psi^\dagger [i\frac{\partial}{\partial t} + \frac{\nabla^2}{2M}] \psi - \frac{C_0}{2} (\psi^\dagger \psi)^2 - \frac{D_0}{6} (\psi^\dagger \psi)^3 + \dots$
- 2** Declaration of regularization and renormalization scheme
 - natural $a_0 \implies$ dimensional regularization and min. subtraction
- 3** Well-defined power counting \implies small expansion parameters
 - use the separation of scales $\implies \frac{k_F}{\Lambda}$ with $\Lambda \sim 1/R \implies k_F a_0$, etc.



$$\mathcal{E} = \rho \frac{k_F^2}{2M} \left[\frac{3}{5} + \frac{2}{3\pi} (k_F a_0) + \frac{4}{35\pi^2} (11 - 2 \ln 2) (k_F a_0)^2 + \dots \right]$$

- cleanly recovers perturbative free-space ERE and in-medium energy density (including logs), plus error estimates

Feynman Rules for EFT Vertices

$$\begin{aligned} \mathcal{L}_{\text{eft}} = & \psi^\dagger \left[i \frac{\partial}{\partial t} + \frac{\vec{\nabla}^2}{2M} \right] \psi - \frac{C_0}{2} (\psi^\dagger \psi)^2 + \frac{C_2}{16} [(\psi \psi)^\dagger (\psi \overleftrightarrow{\nabla}^2 \psi) + \text{h.c.}] \\ & + \frac{C'_2}{8} (\psi \overleftrightarrow{\nabla} \psi)^\dagger \cdot (\psi \overleftrightarrow{\nabla} \psi) - \frac{D_0}{6} (\psi^\dagger \psi)^3 + \dots \end{aligned}$$

$$\begin{aligned} & \begin{array}{c} \text{P}/2 + \mathbf{k} \\ \text{P}/2 - \mathbf{k} \end{array} \begin{array}{c} \text{P}/2 + \mathbf{k}' \\ \text{P}/2 - \mathbf{k}' \end{array} \\ & \begin{array}{c} \text{---} \diagdown \text{---} \\ \text{---} \diagup \text{---} \end{array} = \begin{array}{c} \text{---} \diagdown \text{---} \\ \text{---} \diagup \text{---} \end{array} + \begin{array}{c} \text{---} \diagdown \text{---} \\ \text{---} \diagup \text{---} \end{array} + \begin{array}{c} \text{---} \diagdown \text{---} \\ \text{---} \diagup \text{---} \end{array} + \dots \\ & -i\langle \mathbf{k}' | V_{\text{EFT}} | \mathbf{k} \rangle \quad -iC_0 \quad -iC_2 \frac{\mathbf{k}^2 + \mathbf{k}'^2}{2} \quad -iC'_2 \mathbf{k} \cdot \mathbf{k}' \end{aligned}$$

$$\begin{aligned} & \begin{array}{c} \text{---} \diagdown \text{---} \\ \text{---} \diagup \text{---} \end{array} = \begin{array}{c} \text{---} \diagdown \text{---} \\ \text{---} \diagup \text{---} \end{array} + \dots \\ & -iD_0 \end{aligned}$$

Renormalization

- Reproduce $f_0(k)$ in perturbation theory (Born series):

$$f_0(k) \propto a_0 - ia_0^2 k - (a_0^3 - a_0^2 r_0/2)k^2 + \mathcal{O}(k^3 a_0^4)$$

- Consider the leading potential $V_{\text{EFT}}^{(0)}(\mathbf{x}) = C_0 \delta(\mathbf{x})$ or

$$\langle \mathbf{k} | V_{\text{eft}}^{(0)} | \mathbf{k}' \rangle \implies \begin{array}{c} \swarrow \quad \searrow \\ \bullet \\ \nearrow \quad \nwarrow \end{array} \implies C_0$$

- Choosing $C_0 \propto a_0$ gets the first term. Now $\langle \mathbf{k} | V G_0 V | \mathbf{k}' \rangle$:

$$\begin{array}{c} \swarrow \quad \searrow \\ \bullet \quad \bullet \\ \nearrow \quad \nwarrow \end{array} \implies C_0 M \int \frac{d^3 q}{(2\pi)^3} \frac{1}{k^2 - q^2 + i\epsilon} C_0 \rightarrow \infty!$$

\implies Linear divergence!

Renormalization

- Reproduce $f_0(k)$ in perturbation theory (Born series):

$$f_0(k) \propto a_0 - ia_0^2 k - (a_0^3 - a_0^2 r_0/2)k^2 + \mathcal{O}(k^3 a_0^4)$$

- Consider the leading potential $V_{\text{EFT}}^{(0)}(\mathbf{x}) = C_0 \delta(\mathbf{x})$ or

$$\langle \mathbf{k} | V_{\text{eft}}^{(0)} | \mathbf{k}' \rangle \implies \begin{array}{c} \swarrow \quad \searrow \\ \bullet \\ \nearrow \quad \nwarrow \end{array} \implies C_0$$

- Choosing $C_0 \propto a_0$ gets the first term. Now $\langle \mathbf{k} | V G_0 V | \mathbf{k}' \rangle$:

$$\begin{array}{c} \swarrow \quad \searrow \\ \bullet \quad \bullet \\ \nearrow \quad \nwarrow \end{array} \implies \int^{\Lambda_c} \frac{d^3 q}{(2\pi)^3} \frac{1}{k^2 - q^2 + i\epsilon} \longrightarrow \frac{\Lambda_c}{2\pi^2} - \frac{ik}{4\pi} + \mathcal{O}\left(\frac{k^2}{\Lambda_c}\right)$$

\implies If cutoff at Λ_c , then can absorb into C_0 , but all powers of k^2

Renormalization

- Reproduce $f_0(k)$ in perturbation theory (Born series):

$$f_0(k) \propto a_0 - ia_0^2 k - (a_0^3 - a_0^2 r_0/2)k^2 + \mathcal{O}(k^3 a_0^4)$$

- Consider the leading potential $V_{\text{EFT}}^{(0)}(\mathbf{x}) = C_0 \delta(\mathbf{x})$ or

$$\langle \mathbf{k} | V_{\text{eft}}^{(0)} | \mathbf{k}' \rangle \implies \begin{array}{c} \swarrow \quad \searrow \\ \bullet \\ \nearrow \quad \nwarrow \end{array} \implies C_0$$

- Choosing $C_0 \propto a_0$ gets the first term. Now $\langle \mathbf{k} | V G_0 V | \mathbf{k}' \rangle$:

$$\begin{array}{c} \swarrow \quad \searrow \\ \bullet \quad \bullet \\ \nearrow \quad \nwarrow \end{array} \implies \int \frac{d^D q}{(2\pi)^3} \frac{1}{k^2 - q^2 + i\epsilon} \xrightarrow{D \rightarrow 3} -\frac{ik}{4\pi}$$

Dimensional regularization with minimal subtraction
 \implies only one power of k !

- Dim. reg. + minimal subtraction \implies simple power counting:

$$\begin{aligned}
 & \begin{array}{c} P/2+k \\ \swarrow \quad \searrow \\ \text{---} \text{---} \text{---} \\ \nwarrow \quad \nearrow \\ P/2-k \end{array} = \begin{array}{c} P/2+k' \\ \swarrow \quad \searrow \\ \text{---} \text{---} \text{---} \\ \nwarrow \quad \nearrow \\ P/2-k' \end{array} + \begin{array}{c} P/2+k' \\ \swarrow \quad \searrow \\ \text{---} \text{---} \text{---} \\ \nwarrow \quad \nearrow \\ P/2-k' \end{array} \\
 & iT(k, \cos \theta) = -iC_0 - \frac{M}{4\pi}(C_0)^2 k \\
 & + i\left(\frac{M}{4\pi}\right)^2 (C_0)^3 k^2 - iC_2 k^2 - iC_2' k^2 \cos \theta + \mathcal{O}(k^3)
 \end{aligned}$$

- Matching in free space:

$$C_0 = \frac{4\pi}{M} a_0 = \frac{4\pi}{M} R, \quad C_2 = \frac{4\pi}{M} \frac{a_0^2 r_0}{2} = \frac{4\pi}{M} \frac{R^3}{3}, \quad \dots$$

- Recovers effective range expansion order-by-order with perturbative diagrammatic expansion
 - one power of k per diagram
 - estimate truncation error from dimensional analysis

Noninteracting Fermi Sea at $T = 0$

- Put system in a large box ($V = L^3$) with periodic bc's
 - spin-isospin degeneracy ν (e.g., for nuclei, $\nu = 4$)
 - fill momentum states up to Fermi momentum k_F

$$N = \nu \sum_{\mathbf{k}} 1, \quad E = \nu \sum_{\mathbf{k}} \frac{\hbar^2 k^2}{2M}$$

- Use: $\int F(k) dk \approx \sum_i F(k_i) \Delta k_i = \sum_i F(k_i) \frac{2\pi}{L} \Delta n_i = \frac{2\pi}{L} \sum_i F(k_i)$

- In 1-D:

$$N = \nu \frac{L}{2\pi} \int_{-k_F}^{+k_F} dk = \frac{\nu k_F}{\pi} L \implies \rho = \frac{N}{L} = \frac{\nu k_F}{\pi}; \quad \frac{E}{L} = \frac{1}{3} \frac{\hbar^2 k_F^2}{2M} \rho$$

- In 3-D:

$$N = \nu \frac{V}{(2\pi)^3} \int^{k_F} d^3k = \frac{\nu k_F^3}{6\pi^2} V \implies \rho = \frac{N}{V} = \frac{\nu k_F^3}{6\pi^2}; \quad \frac{E}{V} = \frac{3}{5} \frac{\hbar^2 k_F^2}{2M} \rho$$

- Volume/particle $V/N = 1/\rho \sim 1/k_F^3$, so spacing $\sim 1/k_F$

Energy Density From Summing Over Fermi Sea

- Leading order $V_{\text{EFT}}^{(0)}(\mathbf{x}) = C_0 \delta(\mathbf{x}) \implies V_{\text{EFT}}^{(0)}(\mathbf{k}, \mathbf{k}') = C_0$

$$\mathcal{E}_{\text{LO}} = \frac{C_0}{2} \nu(\nu - 1) \left(\sum_{\mathbf{k}}^{k_F} 1 \right)^2 \propto a_0 k_F^6$$

- At the next order, we get a linear divergence again:

$$\mathcal{E}_{\text{NLO}} \propto \int_{k_F}^{\infty} \frac{d^3 q}{(2\pi)^3} \frac{C_0^2}{k^2 - q^2}$$

- Same renormalization fixes it! **Particles** \longrightarrow **holes**

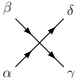
$$\int_{k_F}^{\infty} \frac{1}{k^2 - q^2} = \int_0^{\infty} \frac{1}{k^2 - q^2} - \int_0^{k_F} \frac{1}{k^2 - q^2} \xrightarrow{D \rightarrow 3} - \int_0^{k_F} \frac{1}{k^2 - q^2} \propto a_0^2 k_F^7$$

Feynman Rules for Energy Density at $T = 0$

- $T = 0$ Energy density \mathcal{E} is sum of *Hugenholtz* diagrams
 - same vertices as free space (**same renormalization!**)
- Feynman rules:

1 Each line is assigned conserved $\tilde{k} \equiv (k_0, \mathbf{k})$ and $[\omega_{\mathbf{k}} \equiv k^2/2M]$

$$iG_0(\tilde{k})_{\alpha\beta} = i\delta_{\alpha\beta} \left(\frac{\theta(k - k_F)}{k_0 - \omega_{\mathbf{k}} + i\epsilon} + \frac{\theta(k_F - k)}{k_0 - \omega_{\mathbf{k}} - i\epsilon} \right)$$

2  $\longrightarrow (\delta_{\alpha\gamma}\delta_{\beta\delta} + \delta_{\alpha\delta}\delta_{\beta\gamma})$ (if spin-independent)

3 After spin summations, $\delta_{\alpha\alpha} \rightarrow -\nu$ in every closed fermion loop.

4 Integrate $\int d^4k/(2\pi)^4$ with $e^{ik_0 0^+}$ for tadpoles

5 Symmetry factor $i/(\mathcal{S} \prod_{l=2}^{l_{\max}} (l!)^k)$ counts vertex permutations and equivalent l -tuples of lines

Power Counting

- Power counting rules
 - 1** for every propagator (line): M/k_F^2
 - 2** for every loop integration: k_F^5/M
 - 3** for every n -body vertex with $2i$ derivatives: $k_F^{2i}/M\Lambda^{2i+3n-5}$
- Diagram with V_{2i}^n n -body vertices scales as $(k_F)^\beta$ *only*:

$$\beta = 5 + \sum_{n=2}^{\infty} \sum_{i=0}^{\infty} (3n + 2i - 5) V_{2i}^n.$$


- e.g., $\mathcal{O}(k_F^6)$:  $\implies V_0^2 = 1$

$$\implies \beta = 5 + (3 \cdot 2 + 2 \cdot 0 - 5) \cdot 1 = 6 \implies \mathcal{O}(k_F^6)$$

Power Counting

- Power counting rules
 - 1** for every propagator (line): M/k_F^2
 - 2** for every loop integration: k_F^5/M
 - 3** for every n -body vertex with $2i$ derivatives: $k_F^{2i}/M\Lambda^{2i+3n-5}$
- Diagram with V_{2i}^n n -body vertices scales as $(k_F)^\beta$ *only*:

$$\beta = 5 + \sum_{n=2}^{\infty} \sum_{i=0}^{\infty} (3n + 2i - 5) V_{2i}^n.$$

• e.g.,  $\implies V_0^2 = 2$

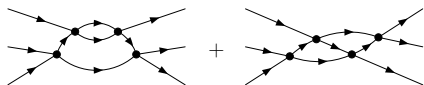
$$\implies \beta = 5 + (3 \cdot 2 + 2 \cdot 0 - 5) \cdot 2 = 7 \implies \mathcal{O}(k_F^7)$$

$T = 0$ Energy Density from Hugenholtz Diagrams

$$\begin{aligned}
 \mathcal{O}(k_F^6) : & \quad \text{[Diagram: two vertices connected by two arcs]} & \quad \frac{E}{V} = & \quad \rho \frac{k_F^2}{2M} \left[\frac{3}{5} + (\nu - 1) \frac{2}{3\pi} (k_F a_0) \right. \\
 \mathcal{O}(k_F^7) : & \quad \text{[Diagram: two vertices connected by three arcs]} + \text{[Diagram: two vertices connected by two arcs with a loop]} & & \quad + (\nu - 1) \frac{4}{35\pi^2} (11 - 2 \ln 2) (k_F a_0)^2 \\
 \mathcal{O}(k_F^8) : & \quad \text{[Diagram: three vertices in a chain connected by two arcs]} + \text{[Diagram: two vertices connected by three arcs with a loop]} & & \quad + (\nu - 1) (0.076 + 0.057(\nu - 3)) (k_F a_0)^3 \\
 & \quad \text{[Diagram: two vertices connected by two arcs with a loop]} + \text{[Diagram: two vertices connected by three arcs]} + \text{[Diagram: two vertices connected by three arcs with a loop]} & & \quad + (\nu - 1) \frac{1}{10\pi} (k_F r_0) (k_F a_0)^2 \\
 & \quad \text{[Diagram: two vertices connected by two arcs with a shaded loop]} + \text{[Diagram: two vertices connected by two arcs with an unshaded loop]} & & \quad + (\nu + 1) \frac{1}{5\pi} (k_F a_p)^3 + \dots \left. \right]
 \end{aligned}$$

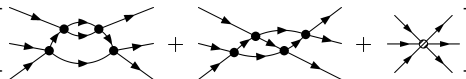
Looks Like a Power Series in k_F ! Is it?

- New **logarithmic** divergences in 3–3 scattering




$$\propto (C_0)^4 \ln(k/\Lambda_c)$$

- Changes in Λ_c **must** be absorbed by **3-body** coupling $D_0(\Lambda_c)$
 $\implies D_0(\Lambda_c) \propto (C_0)^4 \ln(a_0\Lambda_c) + \text{const.}$ [Braaten & Nieto]



$$\frac{d}{d\Lambda_c} \left[\dots \right] = 0 \implies \text{fixes coefficient!}$$

- What does this imply for the energy density?



$$\mathcal{O}(k_F^9 \ln(k_F)) : \dots \propto (\nu-2)(\nu-1) (k_F a_0)^4 \ln(k_F a_0)$$

Summary: Dilute Fermi System with Natural a_0

- The many-body energy density is perturbative in $k_F a_0$
 - efficiently reproduced by the EFT approach
- Power counting \implies error estimate from omitted diagrams
- Three-body forces are **inevitable** in a low-energy effective theory
 - and not unique \implies they depend on the two-body potential
- The case of a natural scattering length is under control for a uniform system
 - What about a finite # of fermions in a trap? (DFT!)
 - **What if the scattering length is not natural?**

Outline

Many-body methods: Selected results

Dilute, natural, Fermi system

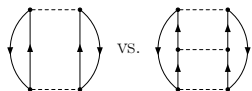
Bethe-Brueckner-Goldstone Power Counting

Teaser for MBPT applied in finite nuclei

Bethe-Brueckner-Goldstone Power Counting

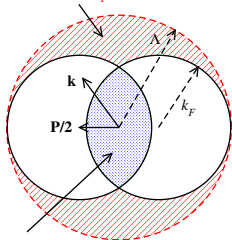
Strong short-range repulsion

\Rightarrow Sum V ladders $\Rightarrow G$

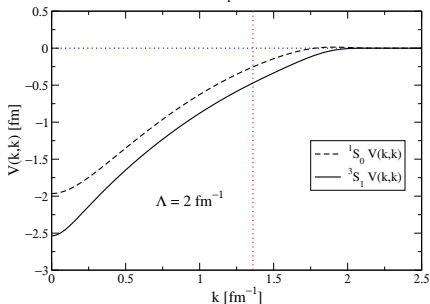
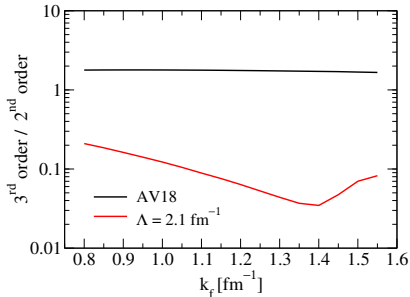


$V_{\text{low } k}$ momentum
dependence + phase space
 \Rightarrow perturbative

$\Lambda: |P/2 \pm k| > k_F$ and $|k| < \Lambda$



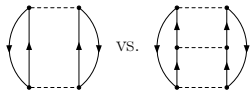
$F: |P/2 \pm k| < k_F$



Bethe-Brueckner-Goldstone Power Counting

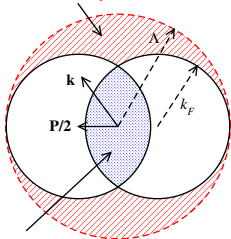
Strong short-range repulsion

\Rightarrow Sum V ladders $\Rightarrow G$

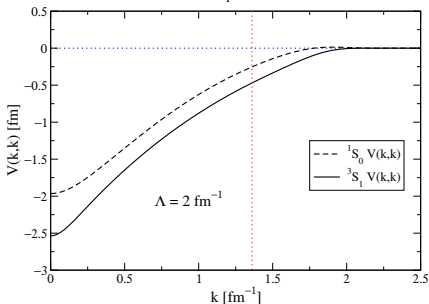
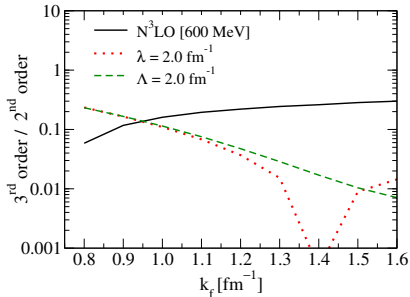


$V_{\text{low } k}$ momentum
dependence + phase space
 \Rightarrow perturbative

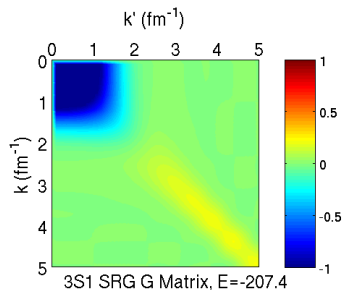
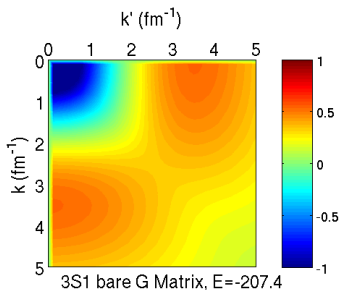
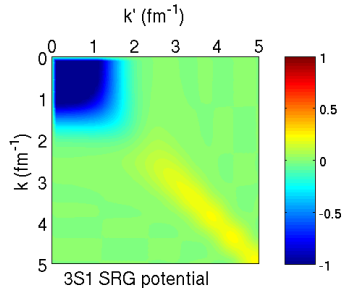
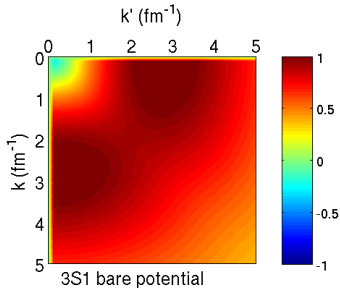
$\Lambda: |P/2 \pm k| > k_F$ and $|k| < \Lambda$



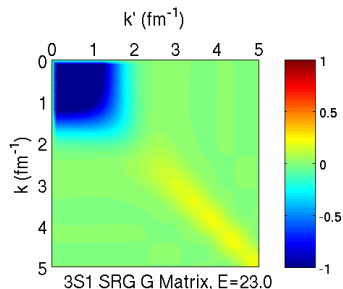
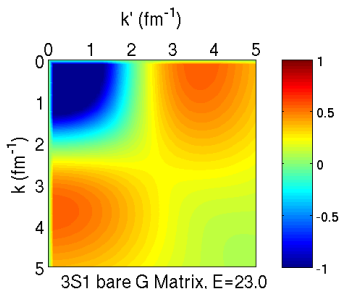
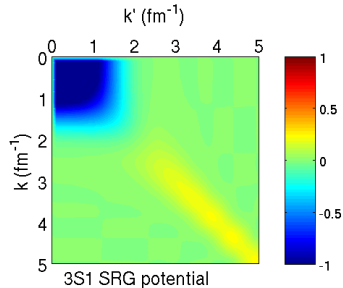
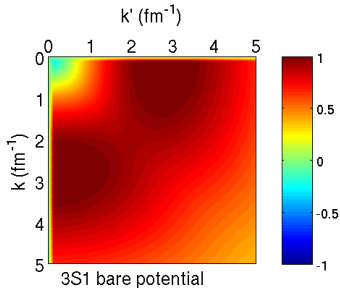
$F: |P/2 \pm k| < k_F$



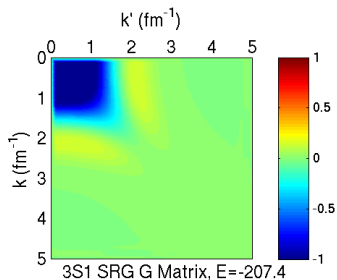
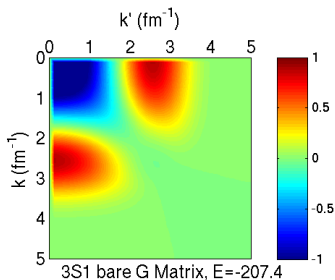
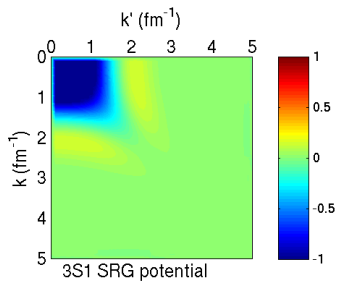
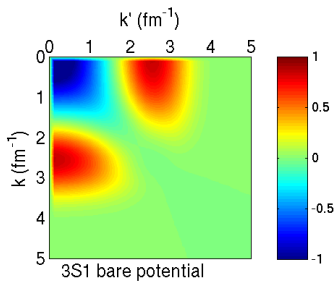
Compare Potential and G Matrix: AV18



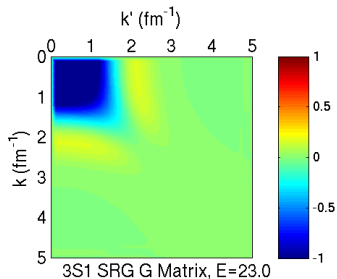
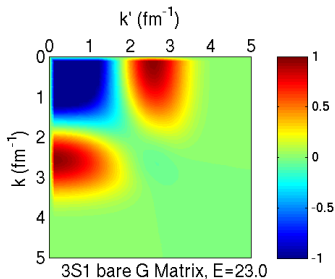
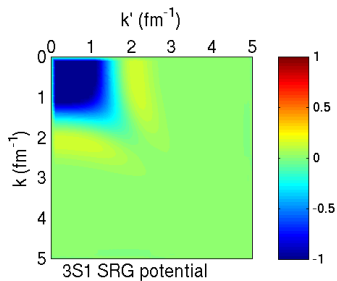
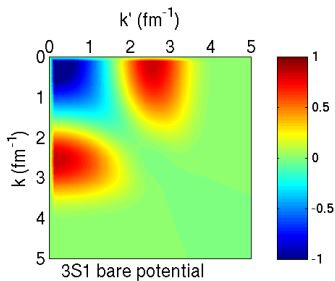
Compare Potential and G Matrix: AV18



Compare Potential and G Matrix: N³LO (500 MeV)

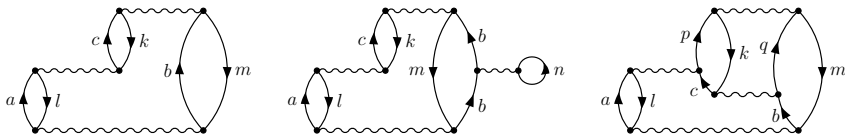


Compare Potential and G Matrix: N³LO (500 MeV)



Hole-Line Expansion Revisited (Bethe, Day, ...)

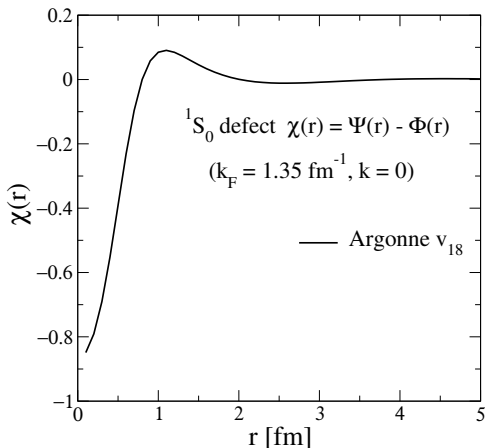
- Consider ratio of fourth-order diagrams to third-order:



- “Conventional” G matrix still couples low- k and high- k
 - no new hole line \implies ratio $\approx -\chi(\mathbf{r} = 0) \approx -1 \implies$ sum all orders
 - add a hole line \implies ratio $\approx \sum_{n \leq k_F} \langle bn | (1/e)G | bn \rangle \approx \kappa \approx 0.15$
 - Low-momentum potentials decouple low- k and high- k
 - add a hole line \implies still suppressed
 - no new hole line \implies also suppressed (limited phase space)
 - freedom to choose single-particle $U \implies$ use for Kohn-Sham
- \implies Density functional theory (DFT) should work!

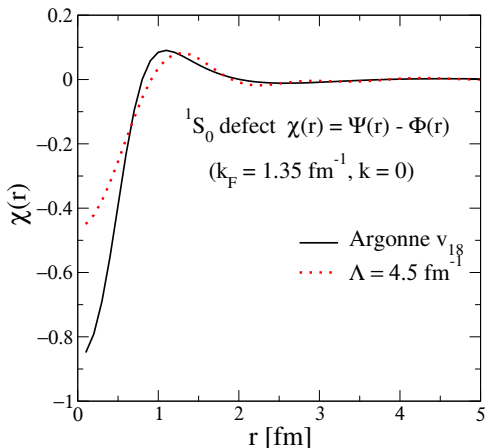
Two-Body Correlations at Nuclear Matter Density

- Defect wf $\chi(r)$ for particular kinematics ($k = 0, P_{\text{cm}} = 0$)
- AV18: “Wound integral” provides expansion parameter



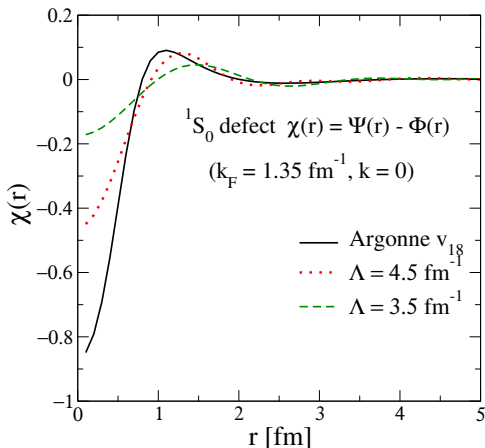
Two-Body Correlations at Nuclear Matter Density

- Defect wf $\chi(r)$ for particular kinematics ($k = 0, P_{\text{cm}} = 0$)
- AV18: “Wound integral” provides expansion parameter



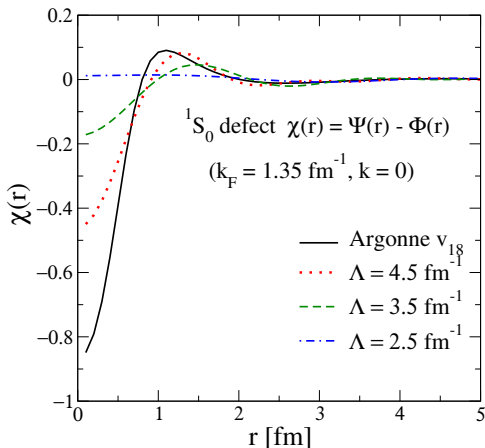
Two-Body Correlations at Nuclear Matter Density

- Defect wf $\chi(r)$ for particular kinematics ($k = 0, P_{\text{cm}} = 0$)
- AV18: “Wound integral” provides expansion parameter



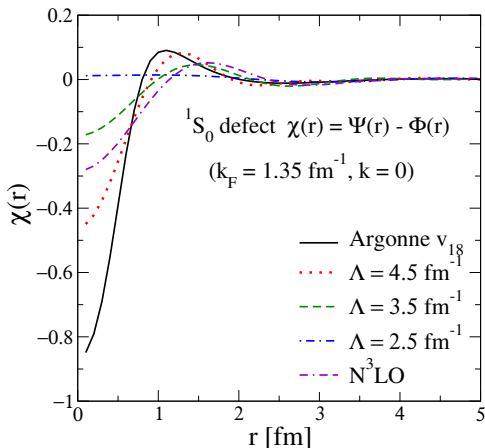
Two-Body Correlations at Nuclear Matter Density

- Defect wf $\chi(r)$ for particular kinematics ($k = 0, P_{\text{cm}} = 0$)
- AV18: “Wound integral” provides expansion parameter
- Extreme case here, but same *pattern* in general
- Tensor (3S_1) \implies larger defect



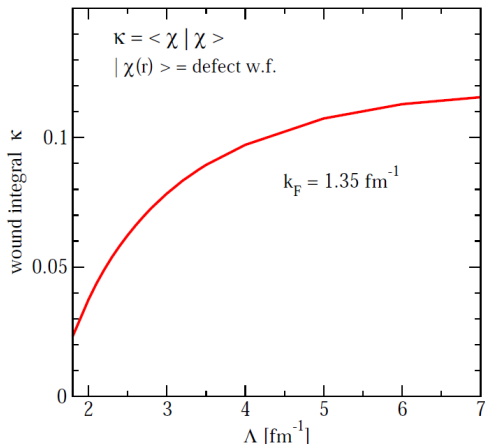
Two-Body Correlations at Nuclear Matter Density

- Defect wf $\chi(r)$ for particular kinematics ($k = 0, P_{\text{cm}} = 0$)
- AV18: “Wound integral” provides expansion parameter
- Extreme case here, but same *pattern* in general
- Tensor (3S_1) \implies larger defect
- Still a sizable wound for $N^3\text{LO}$

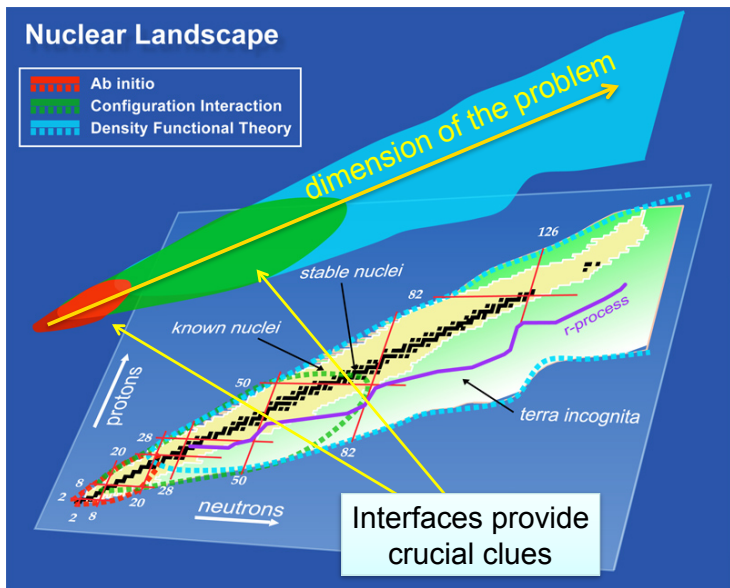


Two-Body Correlations at Nuclear Matter Density

- Defect wf $\chi(r)$ for particular kinematics ($k = 0, P_{\text{cm}} = 0$)
- AV18: “Wound integral” provides expansion parameter
- Extreme case here, but same *pattern* in general
- Tensor (3S_1) \implies larger defect
- Still a sizable wound for $N^3\text{LO}$

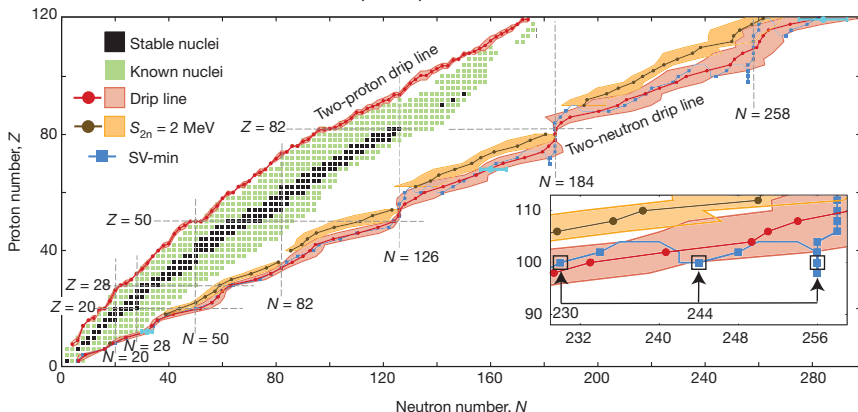


Overlapping theory methods cover all nuclei



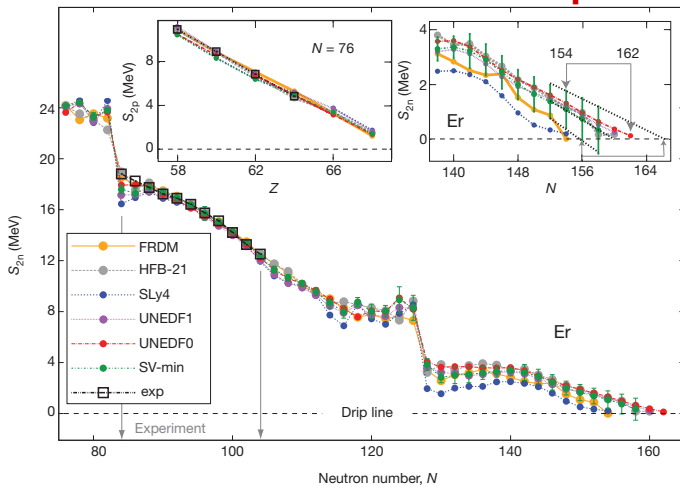
“The limits of the nuclear landscape”

J. Erler et al., Nature **486**, 509 (2012)



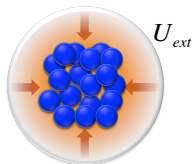
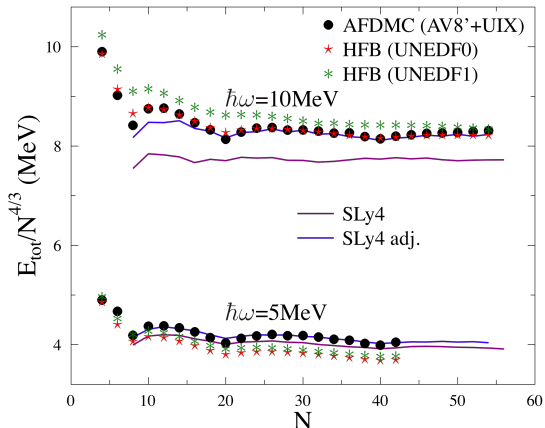
- Proton and neutron driplines predicted by Skyrme EDFs
 - Total: 6900 ± 500 nuclei with $Z \leq 120$ (≈ 3000 known)
 - Estimate systematic errors by comparing models

“The limits of the nuclear landscape”



- Two-neutron separation energies of even-even erbium isotopes
 - Compare different functionals, with uncertainties of fits
 - Dependence on neutron excess poorly determined (cf. driplines)

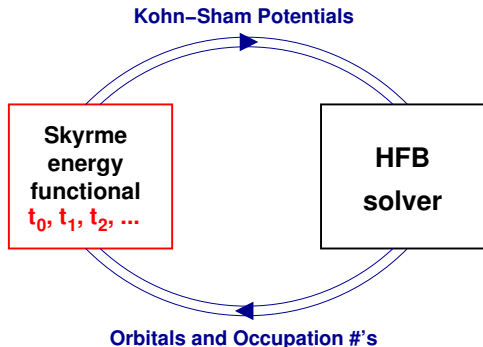
Impact of forces: Use *ab initio* pseudo-data



- Put neutrons in a harmonic oscillator trap with $\hbar\omega$ (cf. cold atoms!)
- Calculate exact result with AFDMC [S. Gandolfi, J. Carlson, and S.C. Pieper, Phys. Rev. Lett. 106, 012501 (2011)] (or with other methods)
- UNEDF0 and UNEDF1 functionals improve over Skyrme SLy4!

Self-consistent Skyrme EDF and beyond

$$\mathcal{E}_{\text{Skyrme}} = \frac{\tau}{2M} + \frac{3}{8}t_0\rho^2 + \frac{1}{16}t_3\rho^{2+\alpha} + \frac{1}{16}(3t_1 + 5t_2)\rho\tau + \frac{1}{64}(9t_1 - 5t_2)|\nabla\rho|^2 + \dots$$



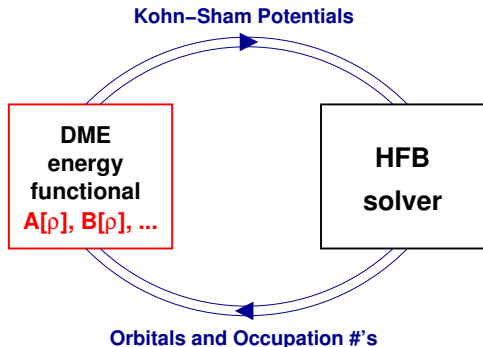
- Kohn-Sham DFT
⇒ iterate to self-consistency
- Looks like dilute, natural functional!
- Low-energy QCD: NDA power counting?
- Use DME to put in pion exchange from χ EFT

Schematic equations to solve self-consistently:

$$V_{\text{KS}}(\mathbf{r}) = \frac{\delta E_{\text{int}}[\rho]}{\delta \rho(\mathbf{r})} \iff \left[-\frac{\nabla^2}{2m} + V_{\text{KS}}(\mathbf{x})\right]\psi_\alpha = \varepsilon_\alpha \psi_\alpha \implies \rho(\mathbf{x}) = \sum_\alpha n_\alpha |\psi_\alpha(\mathbf{x})|^2$$

Self-consistent Skyrme EDF and beyond

$$\mathcal{E}_{\text{Skyrme}} = \frac{\tau}{2M} + \frac{3}{8}t_0\rho^2 + \frac{1}{16}t_3\rho^{2+\alpha} + \frac{1}{16}(3t_1 + 5t_2)\rho\tau + \frac{1}{64}(9t_1 - 5t_2)|\nabla\rho|^2 + \dots$$



- Kohn-Sham DFT
⇒ iterate to self-consistency
- Looks like dilute, natural functional!
- Low-energy QCD:
NDA power counting?
- Use DME to put in pion exchange from χ EFT

Schematic equations to solve self-consistently:

$$V_{\text{KS}}(\mathbf{r}) = \frac{\delta E_{\text{int}}[\rho]}{\delta \rho(\mathbf{r})} \iff \left[-\frac{\nabla^2}{2m} + V_{\text{KS}}(\mathbf{x})\right]\psi_\alpha = \varepsilon_\alpha \psi_\alpha \implies \rho(\mathbf{x}) = \sum_\alpha n_\alpha |\psi_\alpha(\mathbf{x})|^2$$

Outline

Many-body methods: Selected results

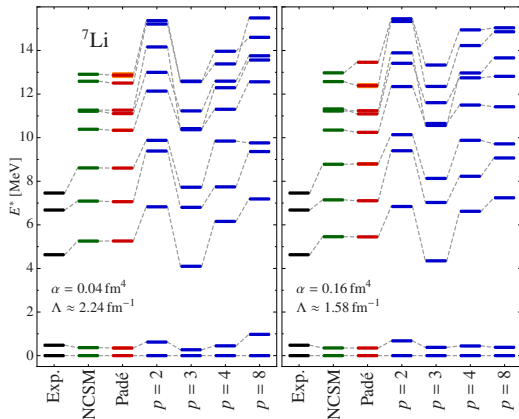
Dilute, natural, Fermi system

Bethe-Brueckner-Goldstone Power Counting

Teaser for MBPT applied in finite nuclei

High-order Rayleigh-Schrödinger MBPT in finite nuclei

- R. Roth et al.
- Excitation energies in ${}^7\text{Li}$
- Degenerate R-S MBPT
- SRG with two resolutions from N^3LO 2NF
- Fixed HO model space



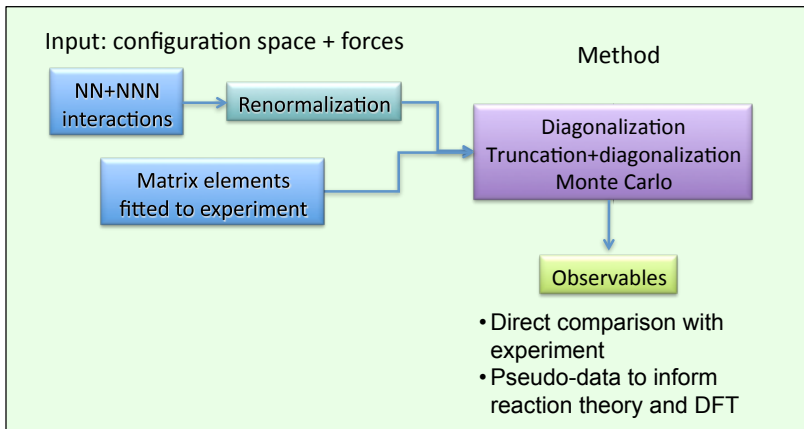
Order $p = 2, 3, 4$, and 8 compared to experiment, exact NCSM calculations, and the Padé resummed result

⇒ note the good agreement of the last two!

The shell model revisited

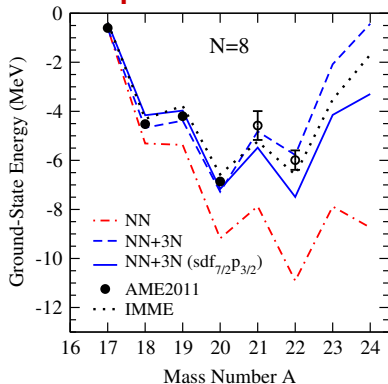
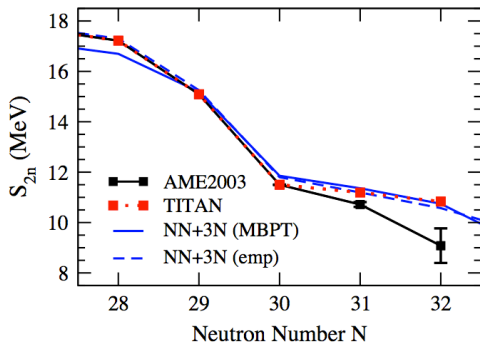
Configuration interaction techniques

- light and heavy nuclei
- detailed spectroscopy
- quantum correlations (lab-system description)



Confronting theory and experiment to both driplines

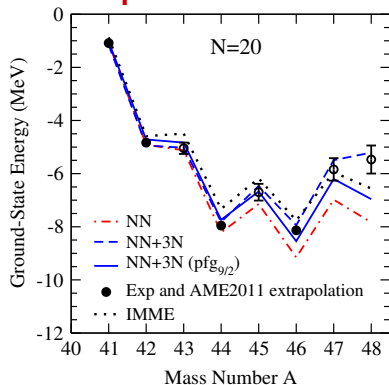
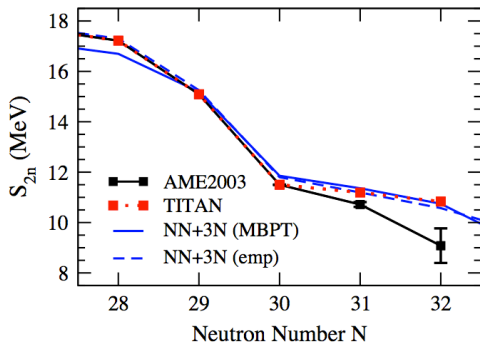
- Precision mass measurements test impact of chiral 3NF
- Proton rich [Holt et al., arXiv:1207.1509]
- Neutron rich [Gallant et al., arXiv:1204.1987]
- Many new tests possible!



- Shell model description using chiral potential evolved to $V_{low k}$ plus 3NF fit to $A = 3, 4$
- Excitations outside valence space included in 3rd order MBPT

Confronting theory and experiment to both driplines

- Precision mass measurements test impact of chiral 3NF
- Proton rich [Holt et al., arXiv:1207.1509]
- Neutron rich [Gallant et al., arXiv:1204.1987]
- Many new tests possible!



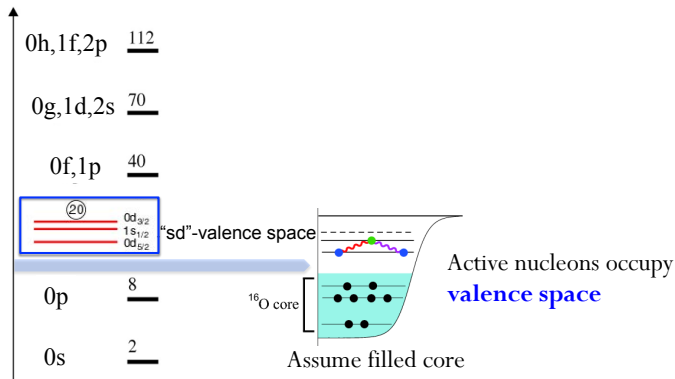
- Shell model description using chiral potential evolved to $V_{low k}$ plus 3NF fit to $A = 3, 4$
- Excitations outside valence space included in 3rd order MBPT

Non-empirical shell model [from J. Holt]

Solving the Nuclear Many-Body Problem

Nuclei understood as many-body system starting from closed shell, add nucleons
Interaction and energies of valence space orbitals from original $V_{\text{low } k}$

This alone does not reproduce experimental data



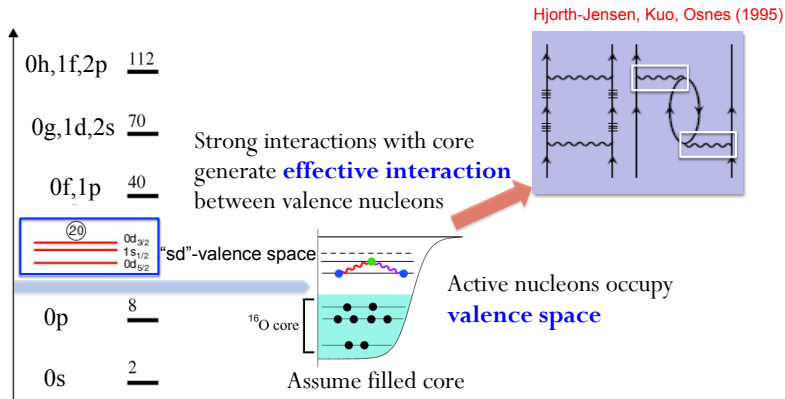
Non-empirical shell model [from J. Holt]

Solving the Nuclear Many-Body Problem

Nuclei understood as many-body system starting from closed shell, add nucleons

Interaction and energies of valence space orbitals from original $V_{\text{low } k}$

This alone does not reproduce experimental data – allow explicit breaking of core



Non-empirical shell model [from J. Holt]

Solving the Nuclear Many-Body Problem

Nuclei understood as many-body system starting from closed shell, add nucleons

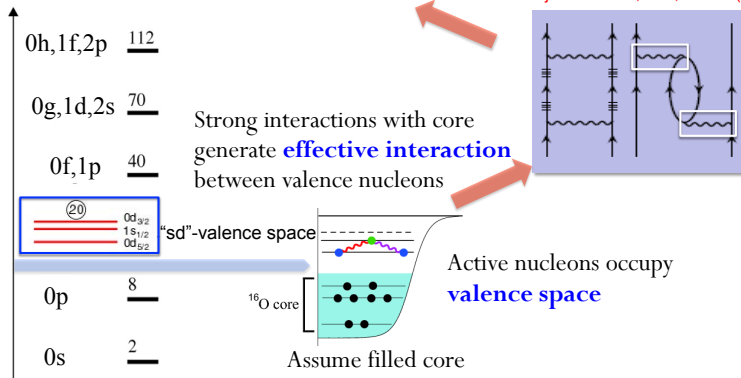
Interaction and energies of valence space orbitals from original $V_{\text{low } k}$

This alone does not reproduce experimental data – allow explicit breaking of core

Effective two-body matrix elements

Single-particle energies (SPEs)

Hjorth-Jensen, Kuo, Osnes (1995)



Chiral 3NFs meet the shell model [from J. Holt]

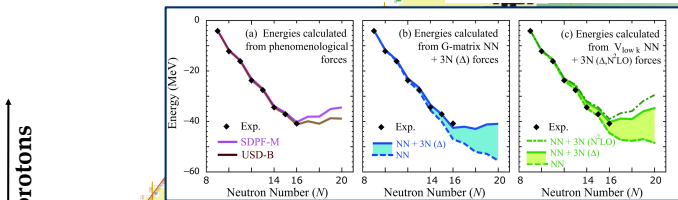
Drip Lines and Magic Numbers: The Evolving Nuclear Landscape

Important in light nuclei, nuclear matter...

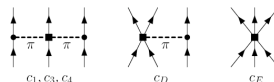
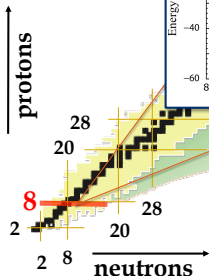
What are the limits of nuclear existence?

How do magic numbers form and evolve?

82 **Heaviest oxygen isotope**



Otsuka, Suzuki, Holt, Schwenk, Akaishi, PRL (2010)



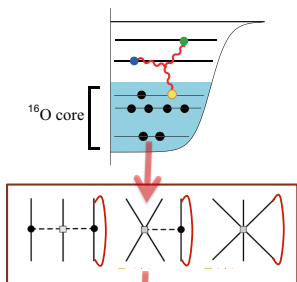
3N forces essential for medium mass nuclei

Chiral 3NFs meet the shell model [from J. Holt]

3N Forces for Valence-Shell Theories

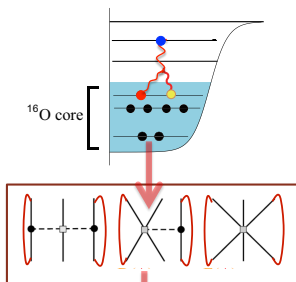
Normal-ordered 3N: contribution to valence neutron interactions

Effective two-body



$$\langle ab | V_{3N,\text{eff}} | a'b' \rangle = \sum_{\alpha = \text{core}} \langle \alpha ab | V_{3N} | \alpha a'b' \rangle$$

Effective one-body



$$\langle a | V_{3N,\text{eff}} | a' \rangle = \frac{1}{2} \sum_{\alpha\beta = \text{core}} \langle \alpha\beta a | V_{3N} | \alpha\beta a' \rangle$$

Combine with microscopic NN: eliminate empirical adjustments

Chiral 3NFs meet the shell model [from J. Holt]

Drip Lines and Magic Numbers: 3N Forces in Medium-Mass Nuclei

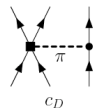
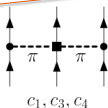
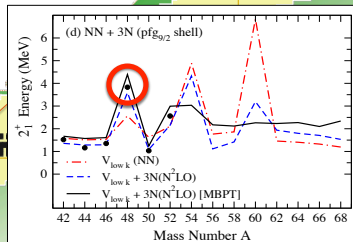
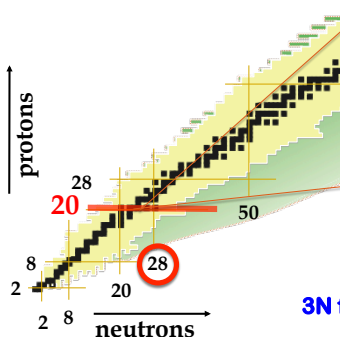
Important in light nuclei, nuclear matter...

What are the limits of nuclear existence?

How do magic numbers form and evolve?

N=28 magic number in calcium

Holt, Otsuka, Schwek,
Suzuki, arXiv:1009.5984



3N forces essential for medium mass nuclei